Science of the Total Environment 481 (2014) 335–342

Contents lists available at ScienceDirect

Science of the Total Environment

journal homepage: www.elsevier.com/locate/scitotenv

Assessment of potential positive effects of nZVI surface modification and concentration levels on TCE dechlorination in the presence of competing strong oxidants, using an experimental design

Delphine Kaifas [a], Laure Malleret [a,*], Naresh Kumar [b], Wafa Fétimi [a], Magalie Claeys-Bruno [c], Michelle Sergent [c], Pierre Doumenq [a]

[a] Aix Marseille Université, CNRS, LCE, FRE 3416, Bâtiment Villemin, Europôle de l'Arbois, Avenue Louis Philibert, BP 80, 13545 Aix en Provence Cedex 4, France
[b] Aix Marseille Université, CNRS, CEREGE, UMR 7330, Europôle de l'Arbois, Avenue Louis Philibert, BP 80, 13545 Aix en Provence Cedex 4, France
[c] Aix Marseille Université, CNRS, LISA, EA 4672, Avenue Escadrille Normandie Niémen, Case 451, 13397 Marseille Cedex 20, France

HIGHLIGHTS

- Assessment of TCE removal efficiency in a mixture of common strong oxidants
- Research of conditions enabling to palliate the competition of Cr(VI) and NO_3^-
- Main effects of and interactions between factors determined by statistical approach
- Improvement by acting on nZVI surface modification or/and concentration levels

GRAPHICAL ABSTRACT

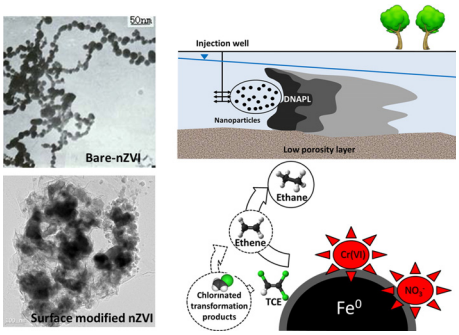

ARTICLE INFO

Article history:
Received 9 December 2013
Received in revised form 12 February 2014
Accepted 12 February 2014
Available online xxxx

Keywords:
Trichloroethylene
Cr(VI)
NO_3^-
Nanoscale zero-valent iron particles
Experimental design
Surface modification

ABSTRACT

Nanoscale zero-valent iron (nZVI) particles are efficient for the remediation of aquifers polluted by trichloroethylene (TCE). But for on-site applications, their reactivity can be affected by the presence of common inorganic co-pollutants, which are equally reduced by nZVI particles. The aim of this study was to assess the potential positive effects of nZVI surface modification and concentration level on TCE removal in the concomitant presence of two strong oxidants, i.e., Cr(VI) and NO_3^-. A design of experiments, testing four factors (i.e. nZVI concentration, nZVI surface modification, Cr(VI) concentration and NO_3^- concentration), was used to select the best trials for the identification of the main effects of the factors and of the factors interactions. The effects of these factors were studied by measuring the following responses: TCE removal rates at different times, degradation kinetic rates, and the transformation products formed. As expected, TCE degradation was delayed or inhibited in most of the experiments, due to the presence of inorganics. The negative effects of co-pollutants can be palliated by combining surface modification with a slight increase in nZVI concentration. Encouragingly, complete TCE removal was achieved for some given experimental conditions. Noteworthily, nZVI surface modification was found to promote the efficient degradation of TCE. When degradation occurred, TCE was mainly transformed into innocuous non-chlorinated transformation products, while hazardous chlorinated transformation products accounted for a small percentage of the mass-balance.

* Corresponding author at: LCE, Bâtiment Villemin, Europôle de l'Arbois, Avenue Louis Philibert, BP 80, 13545 Aix en Provence Cedex 4, France. Tel.: +33 42908415; fax: +33 42908427.
E-mail addresses: delphine.kaifas@etu.univ-amu.fr (D. Kaifas), laure.malleret@univ-amu.fr (L. Malleret), kumar@cerege.fr (N. Kumar), fetimi.wafa_univ.mentouri@hotmail.fr (W. Fétimi), m.claeys-bruno@univ-amu.fr (M. Claeys-Bruno), michelle.sergent@univ-amu.fr (M. Sergent), pierre.doumenq@univ-amu.fr (P. Doumenq).

http://dx.doi.org/10.1016/j.scitotenv.2014.02.043
0048-9697/

1. Introduction

Zero-valent iron (ZVI) particles are well-known today for their efficiency in reducing chlorinated solvents (Roberts et al., 1996; Arnold and Roberts, 2000) and inorganic contaminants (Choe et al., 2000; Ponder et al., 2000) in polluted groundwaters. ZVI particles are commonly used as iron filings within permeable reactive barriers (PRBs) for in-situ plume treatment. However, PRB longevity could be affected by poor clogging and by rapid iron passivation, which reduces their efficiency in treating pollutants (Henderson and Demond, 2007). ZVI has been used to develop another process aiming at palliating these effects: injection of nano-scale zero-valent iron (nZVI) particles in contaminated groundwaters. The aim of this process is to transport nZVI through the aquifer to target contaminated zones using suitable injection techniques, in order to treat in-situ sources of pollutants like dense non-aqueous phase liquid (DNAPL) pools. Thanks to their small size and high surface area, nZVI exhibits higher reactivity than micro-scale ZVI and could migrate along the aquifer porosity in subsurface environment (Zhang, 2003).

Recently, many laboratory studies (Zhang, 2003) have proved the efficiency of nZVI in reducing chlorinated compounds, especially trichloroethylene (TCE) (Liu et al., 2005). However, poor nZVI mobility was reported, due to the aggregation of the particles that causes particle retention by aquifer material and pore clogging (Schrick et al., 2004; Phenrat et al., 2007). Particle transport can be improved by coating the particle surface with polymers or polyelectrolytes (Saleh et al., 2007). Carboxymethyl cellulose (CMC), a water-soluble polysaccharide, aroused much interest as it is cost-effective and environmentally friendly (He et al., 2010; Cirtiu et al., 2011). In addition to the enhancement of mobility, modifying the nZVI surface resulted in protecting the surface by blocking some reactive sites. In terms of in-situ applications, this could help limit nZVI oxidation (Wang et al., 2010) during transport to the target contaminated areas, thus maintaining sufficient particle reactivity for the degradation of pollutants. Moreover, modifying nZVI particles with CMC prevents further agglomeration, thus resulting in smaller particle size and so higher surface area (unpublished data (Kumar, 2013)).

In natural groundwaters, nZVI reactivity and lifetime (Dries et al., 2005; Liu et al., 2007; Reinsch et al., 2010) could be significantly affected by dissolved inorganic ions and reducible species. NO_3^- (Farrell et al., 2000; Schlicker et al., 2000; Liu et al., 2007) and Cr(VI) (Dries et al., 2005; Jeen et al., 2013) are of particular concern because they are strong nZVI-reducible oxidants. Nitrates, mainly from agricultural sources (nitrogen fertilizers, livestock) and wastewater treatment plant effluents, are ubiquitous pollutants of groundwaters. Chromates are also frequent soil and groundwater contaminants in the vicinity of metal working/plating and related facilities, which also use TCE as metal degreaser. Thus, groundwaters in several uncontrolled or abandoned industrial sites are highly contaminated with the joint presence of these three contaminants, as pointed out by the US Environmental Protection Agency (e.g. superfund sites in the San Fernando Valley, CA).

As it obtains electrons from the iron surface, nitrate is reduced intermediately into nitrite and predominantly into ammonium/ammonia. Fe^0 oxidation leads to the reduction of Cr(VI), followed by the precipitation of soluble Cr or mixed Fe/Cr (oxy) hydroxides (Liu et al., 2009). Published research has evidenced the competition between NO_3^- or Cr(VI) and TCE for reactive sites (Farrell et al., 2000; Schlicker et al., 2000; Dries et al., 2005; Sohn et al., 2006; Liu et al., 2007; Kim et al., 2012; Jeen et al., 2013). In addition, the reduction of NO_3^- or Cr(VI) by Fe^0 is a corrosive process and results in the formation on the Fe surface of a film that acts as a barrier to further reactions. This surface passivation can inhibit the reduction of TCE by nZVI (Schlicker et al., 2000; Dries et al., 2005; Liu et al., 2007). These competition phenomena had previously been investigated by running the experiment with TCE in the presence of only one other reducible species and following a one at a time methodology. In this context, our purpose was to assess whether it was possible to achieve satisfactory TCE removal in spite of the negative impact of the concomitant presence of Cr(VI) and NO_3^- by acting on two parameters easily controllable on-site: nZVI surface modification and concentration. An experimental design was implemented to insure information quality and to minimize the number of experiments. Specifically, a fractional factorial design was applied to evaluate the effects of four factors (i.e. nZVI concentration, nZVI surface modification, Cr(VI) concentration and NO_3^- concentration) and of the interactions between two factors. The effects of the factors were studied by measuring the following responses: TCE removal rates at different times, degradation kinetic rates, and the transformation products formed.

2. Materials and methods

2.1. Reagents and chemicals

Trichloroethylene (≥99.5% TCE) and 1,1-dichloroethylene (99% 1,1-DCE) were purchased from Sigma-Aldrich (St Quentin Fallavier, France). Standard stock solutions of *cis*-1,2-dichloroethylene (5 $mg \cdot L^{-1}$ *cis*-DCE), *trans*-1,2-dichloroethylene (5 $mg \cdot L^{-1}$ *trans*-DCE), and vinyl chloride (2 $mg \cdot L^{-1}$ VC) in methanol were obtained from Supelco Analytical (St Quentin Fallavier, France), Toluene-D8 was obtained from Euriso-top (St Aubin, France), potassium chromate (>99.5%), and potassium nitrate (99.6%) from VWR (Fontenay-sous-Bois, France). Sodium carboxymethyl cellulose was purchased from Sigma-Aldrich (St Louis, USA). Standard gases, ethane (≥99.95%), ethene (≥99.95%), acetylene (≥99.6%), H_2 (≥99.999%), and a mix of propane, propene, butane and butene (1% of each in nitrogen) were obtained from Linde Gas (St-Priest, France). Helium (99.9999%), argon (99.999%) and nitrogen (99.999%) were purchased from Air Liquide (Paris, France). Methanol for analysis was purchased from Merck (Darmstadt, Germany).

2.2. Nanoparticles

nZVI particles (NANOFER 25P), with an average particle size of 50 nm, were obtained from NANOIRON (Rajhrad, Czech Republic). They were shipped and stored in dry powder form under nitrogen in an airtight steel container. Before use, the particles were dispersed in a nitrogen purged vessel containing deoxygenated water. A fresh stock solution of bare nZVI (B-nZVI) (92 $g \cdot L^{-1}$) was prepared just before each experiment. Prior to the addition in experimental vials, the nanoparticles were exposed in an ultrasonic bath for 5 min, so as to disperse potentially formed aggregates.

Carboxymethyl cellulose coated nZVI (CMC–nZVI) was prepared by coating the B-nZVI particles with CMC. Coating was carried out by diluting the B-nZVI stock solution into a CMC stock solution ([CMC] = 20 $g \cdot L^{-1}$) prepared in deoxygenated water. The final concentration and content were $[Fe^0] = 46\ g \cdot L^{-1}$ and $[CMC] = 200\ mg \cdot g^{-1}\ Fe^0$, respectively. Then, the CMC–nZVI solution was agitated at 30 rpm (rotating agitation) for 2 h, and placed in an ultrasonic bath for 5 min before spiking.

2.3. Batch experimental set-up

All experiments were set up to investigate the effects of NO_3^- and Cr(VI) on nZVI reactivity towards TCE. Batch experiments were conducted in reactors consisting of 1 L glass bottles capped with a thick PTFE-faced septum. They were prepared in an anaerobic glovebox, where the reactor headspace was initially filled with nitrogen. Each reactor was filled with 1 L of deoxygenated water (resulting in a headspace volume of ~150 mL). The reactors were first spiked with nZVI and then equilibrated for 2 h. Then, appropriate volumes of CrO_4^{2-}, NO_3^- and TCE stock solutions were added to reach the desired concentrations in the reactors (Table A.1). TCE concentration was constant

(10 $mg \cdot L^{-1}$) for all experimental set-ups. During the kinetic monitoring, the reactors were continuously stirred using an orbital shaker (175 rpm) at room temperature (20 °C), in the dark.

2.4. Analysis of TCE and transformation products

The concentrations of TCE and of its chlorinated transformation products (1,1-dichloroethylene, *cis*-dichloroethylene and vinyl chloride) in aqueous phase were determined using a PerkinElmer Clarus 600 gas chromatograph (GC) connected to a PerkinElmer Clarus 600C mass spectrometer (MS) equipped with a PerkinElmer Turbomatrix 40 Trap headspace autosampler. Samples were collected from the aqueous phase from the experimental reactors in glass vials (10 mL) and analyzed in headspace mode, after equilibration for 20 min at 35 °C. The GC was equipped with a split/splitless injector and a PerkinElmer Elite 5-MS column (60 m × 0.25 mm × 1 μm). The injection was performed in split mode (split ratio 1/55 for 5 min) using He as carrier gas at (193 kPa). The oven temperature was programed to start at 30 °C for 5 min, then increased gradually at a rate of 20 °C·min^{-1} up to 180 °C, and maintained for 1.50 min. Ionization was realized by electron impact at 70 eV. Transfer line and source temperatures were 250 °C. Acquisition was performed simultaneously in full scan (m/z = 26–400) and selected ion (m/z = 27, 62, 64 for VC, m/z = 61, 96, 98 for DCE isomers, m/z = 95, 130, 132 for TCE, and m/z = 98, 99, 100 for Toluene-D8) modes. Toluene-D8 was used as an internal standard for analysis. The performances of the method were as follows. The repeatability evaluated by the intra-day residual standard deviation (RSD %, n = 5) was about 2 to 3% for all analytes, except for VC (9.7%). The reproducibility was evaluated for TCE using the inter-day RSD (n = 52) equal to 7.1%. Method detection limits were 1 μg·L^{-1} for *trans*-DCE, 3 μg·L^{-1} for VC, 1,1-DCE and *cis*-DCE, and 5 μg·L^{-1} for TCE, and quantification limits were 3 μg·L^{-1} for *trans*-DCE, 8 μg·L^{-1} for VC, 1,1-DCE and *cis*-DCE, and 15 μg·L^{-1} for TCE. Concentrations of non-chlorinated transformation products in the gas phase were measured by collecting a 100 to 200 μL gas sample from the reactor headspace. Analysis was performed with a PerkinElmer Autosystem XL GC equipped with a split/splitless injector, a PerkinElmer Elite-Q PLOT (30 m × 0.53 mm × 20 μm) column and an FID detector. Argon was used as carrier gas at a constant pressure of 76 kPa. The initial temperature was set at 35 °C for 4 min, then increased at a rate of 10 °C·min^{-1} up to 200 °C, and maintained for 1 min. For the seven gaseous compounds analyzed, the intra-day RSD was less than 2%. Limits of quantification were 0.2 mg·m^{-3} for ethane, ethene and acetylene, 0.5 mg·m^{-3} for propane and propene, and 0.7 mg·m^{-3} for butane and butene.

Both pH and oxido-reduction potential (ORP) were measured with a hand held Multi 340i pHmeter equipped with a SenTix®41 electrode (WTW, Weilheim, Germany). The aqueous phase was regularly monitored (pH, ORP, concentrations of TCE and chlorinated transformation products), from the initial time (addition of contaminants) to the final time (about 500 h). The gas phase (non-chlorinated products) was analyzed at t = 800 h.

2.5. Modeling

TCE kinetic rate constants were determined by fitting the measured TCE concentrations to various models using SigmaPlot version 11.0 (Systat Software Inc., San Jose, USA).

A pseudo first-order model was applied to describe the degradation of TCE by nZVI:

$$C = C_0 . e^{-kt} \quad (1)$$

where C (M) is the concentration at a reaction time t (h), C_0 (M) is the initial concentration, k (h^{-1}) is the first-order rate constant and t (h) is the reaction time. The Neperian logarithmic transformation of Eq. (1) yielded a linear equation, the first-order rate constant k corresponding to the slope estimated by linear regression of the ln-transformed data versus time. k was normalized to the specific surface area of iron (25 $m^2 \cdot g^{-1}$) to enable its comparison with other published values.

2.6. Experimental design

2.6.1. Experimental design methodology

A design of experiments consists of a group of mathematical and statistical techniques that can be used to optimize the organization of the experiments in order to quantify the relationship between the output variables (responses) and the input variables (factors). After identification of the most influential factors, a more detailed study can be performed in order to detect possible interaction effects between the factors, meaning that the influence of some factors could be different according to the value of the other factors.

2.6.2. Experimental factors and domain of interest

Based on previous work reporting on the effect of several parameters on TCE degradation (Song and Carraway, 2005; Liu et al., 2007; Phenrat et al., 2009; Jeen et al., 2013), four experimental parameters, noted as factors U_1, U_2, U_3, U_4, were chosen for this study: nZVI concentration (U_1), nZVI surface modification (U_2), Cr(VI) concentration (U_3), and NO_3^- concentration (U_4). The experiments presented here were designed to mimic the field conditions, so values were chosen according to in-situ application requirements. NANOFER, commercially available nZVI used in several European field application projects, was selected for this study (Mueller et al., 2011). Generally NANOFER is injected in-situ at concentrations ranging from 1 to 5 g·L^{-1}, but nZVI concentrations are very site-specific (Mueller et al., 2011). Saleh et al. (2007) suggested that field scale operations needed at least 3 g·L^{-1} of nZVI. The nZVI concentrations tested here were chosen in this range of values. In addition, as the nZVI surface can be modified with a polymer or a polyelectrolyte to improve particle mobility, we aimed to test both bare nZVI and surface modified nZVI. CMC was chosen for nZVI surface modification because, as reported in recent studies (He et al., 2010; Johnson et al., 2013), it presents many advantages such as low cost and environmental compatibility, and is considered as a potential electron donor for biological communities.

nZVI is a remediation technology particularly appropriate to treat highly polluted areas, such as source area. Hence, TCE concentration was fixed at 10 mg·L^{-1}, which is in the concentration range reported in recent nZVI field-applications (Henn and Waddill, 2006; He et al., 2010; Mueller et al., 2011). As for Cr(VI), concentration levels were chosen based on recent lab and field studies (Xu and Zhao, 2007; Scott et al., 2011; Němeček et al., 2013). Finally, NO_3^- concentration levels were fixed in the range 41 to 411 mg·L^{-1}, typical for natural groundwaters (Dou et al., 2010). Fe^0 was in excess for all experimental conditions, except for the ones with NO_3^- concentration at upper level (400 mg·L^{-1}).

Two levels, coded upper and lower limits ($X_i = -$ and $X_i = +$), were attributed to each factor. The experimental values for these factors, determined in agreement with comments and studies cited above, are described in Table A.1.

2.6.3. Design of experiments

The aim of this study was to evaluate the influence of the four parameters by considering the interaction effects which quantify the change in the effect of one factor when another factor is varied from its low to its high level. We postulated that the result of each experiment is a linear combination of the main effect b_i and interaction effects b_{ij} of each dimensionless variable X_1, X_2, X_3, X_4 (Eq. (2)). Interactions between three or more variables were considered negligible.

$$Y = \beta_0 + \beta_1 X_1 + \beta_2 X_2 + \beta_3 X_3 + \beta_4 X_4 + \beta_{12} X_1 X_2 + \beta_{13} X_1 X_3 + \ldots + \beta_{34} X_3 X_4 + \varepsilon \quad (2)$$

where ε is a random error term representing whatever inaccuracy such model can have. This model is valid only for the tested levels (−1 and +1), and therefore cannot be used for any interpolation or extrapolation. In order to estimate the coefficients at the best, a suitable experimental design was performed, more precisely a D-optimal design with 12 experiments, which is a subset of the experiments from the full factorial design. Table 1 presents the 12 experiments of the design, with replicates for 2 experiments.

3. Results and discussion

The experimental conditions and experimental responses (respectively named U and Y) are presented in Table 1. Experimental responses were TCE removal at t = 500 h (Y1 %), TCE removal at t = 80 h (Y2 %), the molar ratio of transformation products to the initial TCE for non-chlorinated transformation products (Y3 %) and for chlorinated transformation products (Y4 %), the initial pH (Y5), the final pH (Y6),the initial ORP (Y7 mV) and the final ORP (Y8 mV). The measured compounds correspond to TCE transformation products generated through the identified reduction pathways (See Fig. A.1.) (Arnold and Roberts, 2000; Liu et al., 2005; Li et al., 2012). In addition, we did not detect TCE transformation products other than those previously reported. Data concerning the quantification of NO_3^- and transformation products (NO_2^- and NH_4^+) and Cr(VI) are given in supplementary information (Table A.2), but these values were not included among the responses analyzed statistically for the experimental design.

3.1. Correlation between responses

For each response, values were plotted as a function of other responses, in order to evaluate the correlation between responses. Among the possible combinations, only two were significantly correlated. An inverse proportionality was found between the initial pH (Y5) and the initial ORP (Y7), and the final pH (Y6) and the final ORP (Y8) (Fig. A.2), indicating that these responses are controlled by the same factors and interactions.

3.2. TCE removal, kinetic rates and effects of factors

TCE removal rates measured after 80 h and at the end of the experiment (500 h) are presented in Fig. 1a.

Profiles of TCE removal rate at t = 80 h varied, depending on the experimental conditions (Table 1), and a high TCE removal was observed in only three experimental trials: Runs 4, 9 and 15 with 70.7%, 53.8%, and 76.5%, respectively. For the other experimental setups, values were significantly lower (<24%) or even zero. These results indicate that one (or several) tested factor(s) had an effect on the TCE degradation at the early stages of the experiment. Results for TCE removal rates at t = 500 h showed a complete removal for Runs 2, 4, 8, 9 and 15. This result is not surprising for Runs 4, 9 and 15, since the corresponding TCE removal rates at t = 80 h were high, but it was not the case for Runs 2 and 8. Values were significantly lower for the other experimental setups (6.1–39.1%). These results suggest that one (or more) factor(s) could affect the TCE removal kinetic rates.

Degradation kinetic rates were evaluated for runs with a complete TCE removal (Runs 2, 4, 8, 9 and 15). Data were plotted as the Neperian logarithm of the TCE concentration at a reaction time t to the initial TCE concentration ($\ln([TCE]_t / [TCE]_0)$) versus reaction time (Fig. 1b) and fitted with a pseudo-first order model. Different trends were observed. First, identical profiles were obtained for Runs 4 and 15, and data were well fitted with the proposed model with, k_{TCE} = 0.022 h^{-1} (r^2 = 0. 980) and k_{TCE} = 0.021 h^{-1} (r^2 = 0.993), respectively. Run 9, however, showed a lower initial kinetic rate (k_{TCE} = 0.009 h^{-1}, r^2 = 0.966), with a slight increase in the slope occurring at about 170 h (k_{TCE} = 0.044 h^{-1}, r^2 = 0.951). Finally, Runs 2 and 8 showed a plateau at the beginning of the experiment, and degradation started at t = 150 h (k_{TCE} =0.029 h^{-1}, r^2 = 0.999) and 130 h (k_{TCE} = 0.008 h^{-1}, r^2 = 0.995), respectively. These differences indicate that TCE removal may be delayed at the beginning of the experiment, and could occur at different kinetic rates. These results are in agreement with the available literature studies, which showed inhibited or delayed TCE degradation and lower kinetic rates in the presence of NO_3^- or Cr(VI) (Cho and Park, 2005; Dries et al., 2005; Liu et al., 2007).

In order to quantify the main interaction effects, datasets were statistically treated with a synergic model (Eq. (2)), and coefficients (b_i and b_{ij}) were estimated using a multilinear regression. Results are presented in Fig. 2.

Fig. 2a shows that the nZVI concentration (U_1) and nZVI surface modification (U_2) were the most significant individual factors affecting TCE removal at t = 500 h. Both factors showed a positive influence (b_1 = 31.3 and b_2 = 32.76), which means that the coded levels Xi = +, corresponding to nZVI concentration = 2.8 g·L^{-1} and nZVI surface modification = CMC–nZVI, increase the TCE removal at t = 500 h. On the other hand, TCE removal rate at t = 80 h was affected by an interaction between these factors (Fig. 2b) (b_{1-2} = 10.56), indicating that the best condition to maximize TCE removal at t = 80 h depends on the level of both factors (U_1 and U_2), and changing the level of one of

Table 1
Experimental design and experimental results.

Run number	Design of experiments				Experimental conditions				Experimental results							
	X_1	X_2	X_3	X_4	U_1 (g·L^{-1})	U_2	U_3 (mg·L^{-1})	U_4 (mg·L^{-1})	Y1 (%)	Y2 (%)	Y3 (%)	Y4 (%)	Y5	Y6	Y7 (mV)	Y8 (mV)
1	−1	−1	1	−1	0.9	B-nZVI	20	40	20.0	0	0.6	0	8.3	8.6	−90	−104
2	1	−1	−1	−1	2.8	B-nZVI	3	40	100	19.4	98.5	1.86	9.3	10.3	−155	−220
3	−1	1	−1	1	0.9	CMC–nZVI	3	400	13.1	14.7	10.1	0.79	9.9	11.4	−186	−277
4	1	1	1	1	2.8	CMC–nZVI	20	400	100	70.7	90.8	0.75	10.4	11.6	−217	−293
5	−1	−1	1	1	0.9	B-nZVI	20	400	15.7	12.8	0.2	0	9.1	9.0	−141	−153
6*	1	−1	−1	1	2.8	B-nZVI	3	400	23.5	14.5	1.5	0.03	9.7	10.5	−178	−226
7*	1	−1	−1	1	2.8	B-nZVI	3	400	29.6	12.4	0.1	0	9.7	9.1	−175	−148
8	−1	1	−1	−1	0.9	CMC–nZVI	3	40	100	23.5	83.0	3.42	10.3	10.5	−182	−230
9	1	1	1	−1	2.8	CMC–nZVI	20	40	100	53.8	86.1	3.11	10.4	10.9	−219	−252
10	−1	−1	−1	−1	0.9	B-nZVI	3	40	6.1	2.4	1.0	0	9.4	8.8	−159	−147
11*	1	−1	1	−1	2.8	B-nZVI	20	40	39.1	12.8	22.0	1.06	10.3	10.5	−213	−227
12*	1	−1	1	−1	2.8	B-nZVI	20	40	17.4	11.5	18.8	0.04	10.2	10.2	−208	−210
13*	1	−1	1	−1	2.8	B-nZVI	20	40	22.6	7.9	**	**	10.0	10.0	−194	−197
14	−1	1	1	1	0.9	CMC–nZVI	20	400	30.4	13.5	33.5	0	10.4	10.8	−217	−239
15	1	1	−1	1	2.8	CMC–nZVI	3	400	100	76.5	81.3	0.84	10.1	11.6	−200	−291

U_1 = nZVI concentration; U_2 = nZVI surface modification; U_3 = Cr(VI) concentration; U_4 = NO_3^- concentration; Y1 = TCE removal at t = 500 h (%); Y2 = TCE removal at t = 80 h (%); Y3 = molar ratio of non-chlorinated transformation products to initial TCE (%) at t = 800 h; Y4 = molar ratio of chlorinated transformation products to initial TCE (%) at t = 800 h; Y5 = initial pH; Y6 = final pH; Y7 = initial ORP (mV); Y8 = final ORP (mV). For Y3 and Y4, values were corrected by the number of carbon. *Runs highlighted with an asterisk (column 1) correspond to replicates. **Outlier values, not taken into account for data treatment.

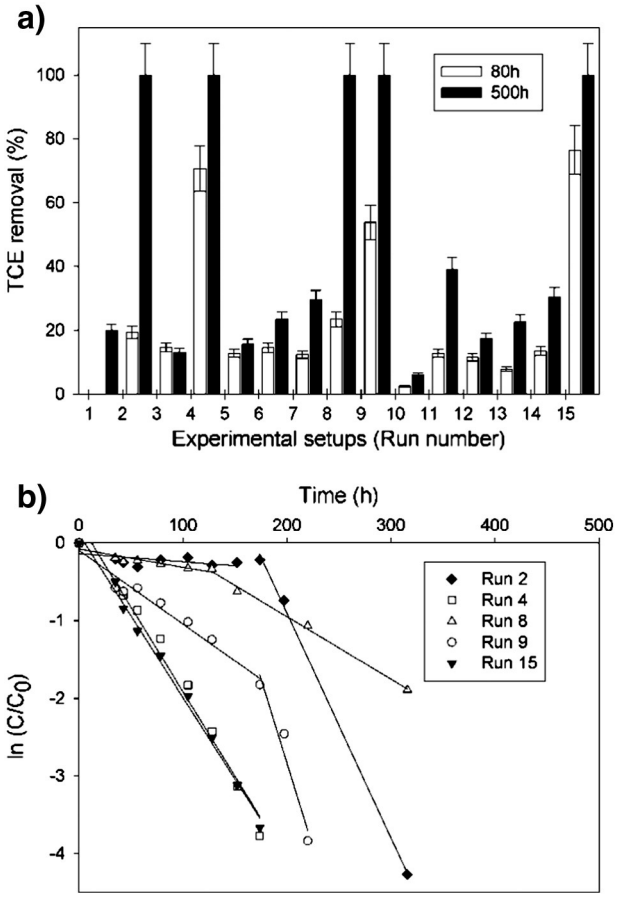

Fig. 1. TCE removal rate (%) at t = 80 h and t = 500 h for each experimental set-up (Runs in Table 1) (a). TCE degradation for different experimental set-ups as the Neperian logarithm of the TCE concentration at a reaction time t $[TCE]_t$ to the initial TCE concentration $[TCE]_0$ versus reaction time (b). Lines represent a pseudo-first order fit.

these factors results in a change in the overall effect. Fig. 2c, which details this interaction, indicates that TCE removal rate at t = 80 h was slightly improved when only one of these factors was increased from level $X_i = -$ to level $X_i = +$, while a significantly higher removal was achieved if both factors were at level $X_i = +$ (nZVI concentration = 2.8 $g \cdot L^{-1}$ and nZVI surface modification = CMC–nZVI).

Improving the final TCE removal by increasing nZVI concentration can be accounted for by the increase in the amount of reactive sites available for TCE reduction. These results are consistent with those of Song and Carraway (2005) and Wang and Zhou (2010), who suggested a linear relation between nZVI dose and contaminant reduction.

It was not expected that the effect of nZVI surface modification would be the improvement of TCE removal, with regard to the results of Phenrat et al. (2009), which demonstrated a limitation of polyelectrolyte modified nZVI reactivity towards TCE. On the one hand, CMC layers could concentrate TCE, due to its hydrophobic character, but they limit the mass transfer to the nZVI surface reactive sites (Phenrat et al., 2009). On the other hand, CMC is negatively charged at pH > 5.5 (Pensini et al., 2011), which could cause electrostatic repulsion of anions, hence promoting the degradation of TCE rather than that of nitrate and Cr(VI). Accordingly, it has been reported that Cr(VI) removal by nZVI was improved by positively charged nanoparticles, due to the attraction of negative Cr(VI) ions, and was inhibited by negatively charged particles, due to the repulsion of negative Cr(VI) ions (Lv et al., 2011). Secondly, it was necessary to increase both factors U_1 and U_2 to significantly improve TCE removal in the early stages of the experiment (t = 80 h). This result could be explained by the fact that the reduction kinetic rates are higher for Cr(VI) and NO_3^- than for TCE (Alowitz and Scherer, 2002), and suggests that competition for reactive site occurs at the beginning of the experiment. Using nZVI in high concentration and CMC surface modification could limit these competition effects.

TCE removal rate at t = 80 h was affected by an interaction between nZVI surface modification and Cr(VI) concentration (Fig. 2b) ($b_{2-3} = -5.03$). Best removal rates were obtained for CMC-modified nZVI and low Cr(VI) concentration (Fig. 2d). Nevertheless, for both Cr(VI) concentrations (3 and 20 $mg \cdot L^{-1}$), using CMC–nZVI rather than B-nZVI improved TCE degradation. These results suggest that surface modification by CMC could limit the competition between TCE and Cr(VI).

Finally, TCE removal rates at t = 80 h and 500 h were affected by an interaction between Cr(VI) and NO_3^- concentrations (Fig. 2a and b) (b_{3-4}). Optimum conditions were obtained for low concentrations of both ions (Figs. 2e and A.3), and increasing the concentration of one of them led to decreased TCE removal rates, suggesting competition between both inorganics. This effect is more pronounced at 500 h (Fig. 2e). For TCE removal at t = 500 h, the effect of NO_3^- seemed to be inhibited by high Cr(VI) concentration. This result could suggest higher reduction kinetic rates for Cr(VI). Studies on the individual effects of NO_3^- and Cr(VI) on nZVI oxidation have shown that nZVI were passivated by both ions (Reinsch et al., 2010; Suzuki et al., 2012). NO_3^- causes the formation of a protective shell (magnetite) (Reinsch et al., 2010), and Cr(VI) is reduced to Cr(III), then precipitates and is incorporated into a Fe(III)–Cr(III) oxide shell (Suzuki et al., 2012). The formation of these oxide shells leads to the passivation of the iron surface and inhibits electron transfers from the Fe^0 core, leading to a decrease in reactivity (Li et al., 2008; Suzuki et al., 2012; Jeen et al., 2013). Furthermore, kinetic rates are higher for Cr(VI) than for NO_3^- (Alowitz and Scherer, 2002), and thus Cr(VI) is probably the first pollutant which reacts with nZVI. High Cr(VI) concentrations probably cause a passivation of the iron particle surface, affecting NO_3^- effect and nZVI reactivity towards TCE. However, further experiments are necessary to confirm this hypothesis.

3.3. TCE degradation transformation products and effects of factors

Chlorinated transformation products were measured in the aqueous phase at t = 500 h, and non-chlorinated transformation products were measured in the gas phase at t = 800 h, for each experimental setup (Table 1). The displayed values correspond to the molar ratio of transformation products to initial TCE (%) for non-chlorinated transformation products (Y3 %) and for chlorinated transformation products (Y4 %). Values were corrected by the number of carbon atoms in the molecule considered, i.e. 1 mol of butane corresponds to 2 mol of TCE.

TCE was first transformed into ethane (major), ethene and coupling products with 3 or 4 carbons (propane, propene, butane and butene, ΣC_3–C_4) (minors), which are mainly present in the gas phase (Fig. 3).

Traces of acetylene were also detected in some cases (not shown). In addition, small amounts of chlorinated products (*cis*-DCE (major), 1,1-DCE (minor) and vinyl chloride (traces)) were quantified, mainly in the aqueous phase, and were generally not detected any more before the end of the experiment. This observation is consistent with other studies on TCE dechlorination with different ZVI or nZVI particles, which proposed β-elimination as the main dechlorination pathway, with the predominant formation of ethane and ethene (Roberts et al., 1996; Liu et al., 2005) (Fig. A.1).

As presented in Fig. 3, the amounts of the main transformation products formed were significantly different, depending on the experimental setup. To characterize the mechanisms of TCE removal, the decrease in TCE concentration was compared with the appearance of transformation products generated by reduction according to the pathways presented in Fig. A.1. For that purpose, the carbon mass balance (CMB) was calculated as the ratio (%) of the sum of the final transformation products quantified to the quantity of TCE removed. Results fall into three broad categories. For the first one (Runs 2, 4, 8, 9, and 15) we

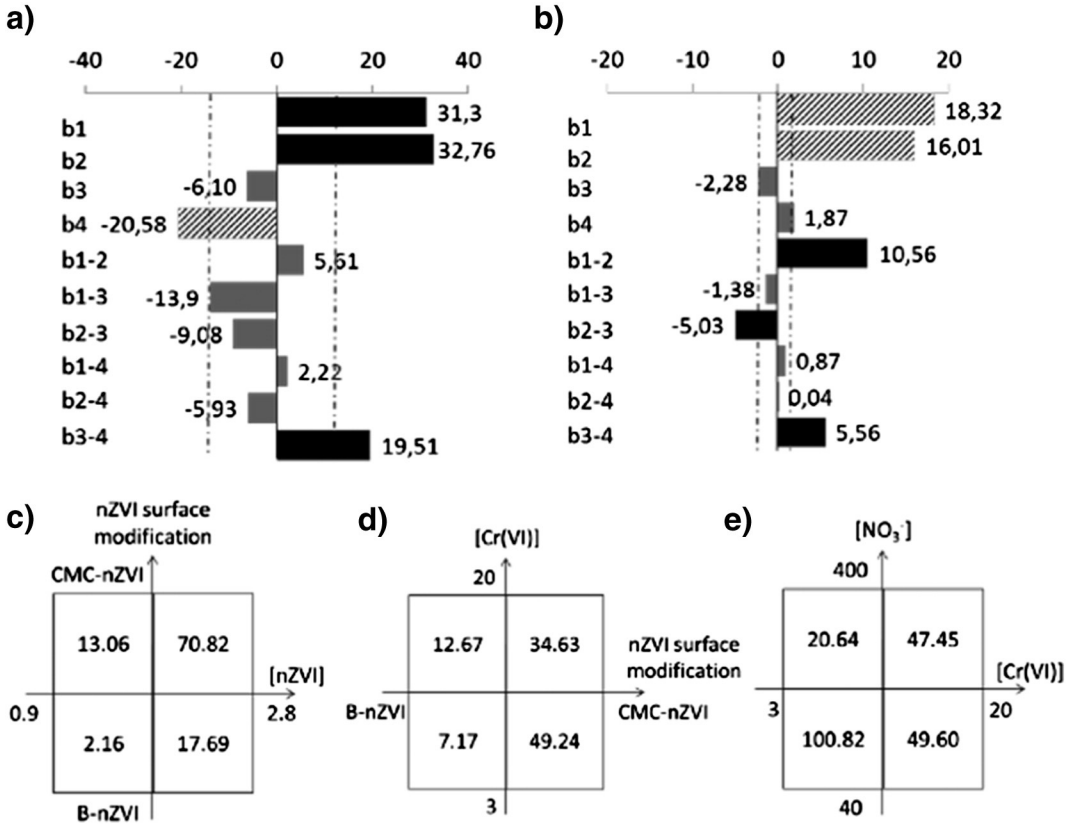

Fig. 2. Effects of nZVI concentration (U_1), nZVI surface modification (U_2), Cr(VI) concentration (U_3) and NO_3^- concentration (U_4) on TCE removal rate at t = 500 h (Y2) (a) and t = 80 h (Y1) (b). b_i represents the effect of the factor U_i on the response (Y_1). A positive value indicates that the factor increases the response when it is changed from level (−) to level (+). A negative value indicates that the factor decreases the response when it is changed from level (−) to level (+). Effect is considered significant when the value is higher than the significance limits (dotted lines). b_{ij} represents the interaction between the factors U_i and U_j. If b_{ij} is significant, individual effects (b_i and b_j) are not considered (hatched bars). Graphs of interaction effects on TCE removal rate at t = 80 h (c and d) and TCE removal at t = 500 h (e): axes represent the interacting factors, and numerical values represent the response for the corresponding conditions. Reading the interaction graph from left to right, or from bottom to top means increasing the factor from level (−) to level (+).

observed complete TCE removal with a well-balanced CMB (>80%). This indicates that TCE removal was efficient and obviously due to reductive dechlorination. The second category (Runs 3, 11, 12, and 14) showed incomplete TCE removal, also due to reductive dechlorination since CMB was higher than 80% (except for Run 11, CMB = 56%), reflecting less favorable conditions for TCE reduction than the first category of experimental runs. Ethane, ethene and coupling product (ΣC_3–C_4) relative abundances were quite similar, except for Runs 9 and 14, where ethane was dominant at the expense of ethene. Conversely, the third category (Runs 1, 5, 6, 7, 10 and 13) showed efficient removal of TCE but poor CMB (<20%), which could suggest that TCE removal was more controlled by sorption phenomena or volatilization losses. In addition, low TCE removal values showed that TCE reduction was strongly affected by some of the tested factors, to the point of inhibiting the reaction.

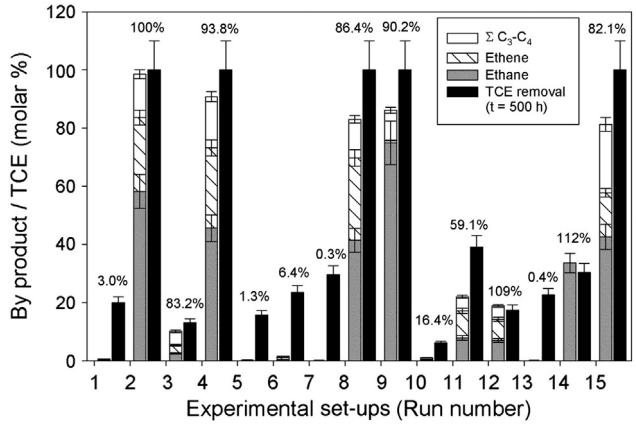

Fig. 3. Relative abundance of the transformation products detected at t = 800 h (%) and comparison with TCE removal rate at t = 500 h, for each experimental set-up. For easier reading, only main transformation products (non-chlorinated products) were reported. Values represent the molar ratio of transformation product to initial TCE, for ethane, ethene and coupling products (ΣC_3C_4), and were corrected by the number of carbon, i.e. 1 mol of butane corresponds to 2 mol of TCE. Numbers represent carbon mass balance (CMB) for each experimental set-up, which includes chlorinated transformation products.

Concerning NO_3^- (see Table A.2), as for TCE, we obtained a total removal for some conditions (Runs 1, 2, 4, 8, 9 and 15) with a satisfactory N mass balance (NMB) (Runs 1, 2, 4 and 15), implying a reduction mechanism for nitrate. For some experiments, as for TCE, the poor NMB probably reflects sorption phenomena. Chromium removal (see Table A.2) was complete and very fast, except for conditions 5 and 1 (not determined). Run 5 seemed to correspond to the poorest conditions in term of TCE, NO_3^- and Cr(VI) removal.

3.3.1. Non-chlorinated transformation products

The conversion of TCE to non-chlorinated transformation products was mainly affected by the nZVI surface modification (U_2), which enhances the production of non-chlorinated transformation products (Table A.2). As shown above, using CMC-modified nZVI enhanced the reduction of TCE, and therefore its conversion to non-chlorinated transformation products. As observed for TCE removal rates, the formation of non-chlorinated products was impacted by an interaction between Cr(VI) concentration (U_3) and NO_3^- concentration (U_4) with a b_{3-4} value of 21.86 (Table A.3 and Fig. 4), which gave rise to a higher

production of non-chlorinated transformation products for low concentrations of both ions.

Increasing NO_3^- concentration for high Cr(VI) concentration did not significantly change the response value. These results suggest that Cr(VI) and NO_3^- competed with TCE but could also compete with each other. Furthermore, Cr(VI) could be the most efficient competitor when present at high concentration, even if the ratio NO_3^- to TCE is significantly larger than the ratio Cr(VI) to TCE.

A lower interaction ($b_{1-3} = -11.98$) was also found between nZVI concentration (U_1) and Cr(VI) concentration (U_3) (Fig. 4). Higher amounts of transformation products were produced for nZVI concentration at level Xi = + and Cr(VI) concentration at level Xi = −. However, when Cr(VI) concentration was at level Xi = +, an increase in nZVI concentration resulted in less impact.

3.3.2. Chlorinated transformation products

The production of chlorinated transformation products was only controlled by nZVI surface modification (U_2) and NO_3^- concentration (U_4) with an interaction effect (Table A.3). Higher chlorinated transformation product concentrations were measured for CMC–nZVI and low NO_3^- concentration (Fig. A.4). Modifying one of the two factors led to a decrease in the production of chlorinated transformation products. It is noteworthy that increased chlorinated transformation product concentration did not necessarily reflect an improvement in the TCE degradation rate, but could suggest that the chlorinated transformation products accumulated more and longer due to low kinetic rates and/or inhibition of their degradation. Nevertheless, as discussed above, NO_3^- is known to form a passivating layer around the particles, which decrease the electron transfer from the core, and decrease or inhibit the TCE reduction and thus the formation and subsequent reduction of its transformation products (Liu et al., 2007; Reinsch et al., 2010; Suzuki et al., 2012). Further experiments, including particle surface characterization, would be necessary to determine how passivation affects the accumulation of chlorinated transformation products.

4. Physico-chemical properties

Initial conditions (pH and ORP) were measured a few minutes after spiking the contaminants, and final conditions (pH and ORP) were measured at t = 500 h. Values are given in Table 1. From this table it can be noticed that initial conditions (Y5 and Y7) were alkaline (pH = 8.3 to 10.4) and reductive (ORP = −90 to −219 mV), due to the corrosion of ZVI by water (Eq. (3)) (Chen et al., 2001).

$$Fe^0 + 2H_2O \rightarrow Fe^{2+} + H_2\uparrow + 2OH^-. \quad (3)$$

As shown by the final pH and ORP values (Y6 and Y8), the conditions became more alkaline and reductive at the end of the experiments. This could be explained by the reduction of NO_3^- and Cr(VI) by nZVI, which subsequently leads to a decrease in ORP and to the formation of hydroxyl ions, as described by Melitas et al. (2001) and Yang and Lee (2005):

$$4Fe^0 + NO_3^- + 7H_2O \rightarrow 4Fe^{2+} + NH_4^+ + 10OH^- \quad (4)$$

$$Fe^0 + CrO_4^{2-} + 4H_2O \rightarrow Cr(OH)_3 + Fe(OH)_3 + 2OH^-. \quad (5)$$

The variation in the pH and ORP values between batch experiments may be attributed to the variation in the tested factors. The model coefficients estimated by multilinear regression are given in Table A.4.

The initial pH and ORP values were affected by an interaction between nZVI concentration (U_1) and nZVI surface modification (U_2) (Fig. A.5). For B-nZVI, increasing nZVI concentration led to increased pH values and decreased ORP values, due to the typical corrosion of iron by water (Eq. (1)) (Chen et al., 2001). This effect was not observed for CMC–nZVI, suggesting that coating nZVI surface with CMC could protect iron from the initial corrosion by water (Wang et al., 2010). Given that CMC–nZVI was post-synthesis modified, hydroxyl ions could have been generated by reduction of traces of dissolved oxygen (Eq. (6)) present in the CMC stock solution.

$$2Fe^0 + 4H^+ + O_2 \rightarrow 2Fe^{2+} + 2H_2O. \quad (6)$$

Another interaction affecting the initial pH and ORP was found between nZVI concentration (U_1) and Cr(VI) concentration (U_3) (Fig. A.5). The results deduced from the experimental design show that the initial conditions are not only due to the corrosion by water but also due to the reduction of chromate. This can be justified by other studies demonstrating that the latter reaction is very fast (several minutes even at pH 8) (Li et al., 2008; Liu et al., 2010).

Increasing nZVI concentration for Cr(VI) up to 20 $mg \cdot L^{-1}$ results in a more efficient Cr(VI) reduction reflected by the more alkaline and reductive conditions (see Eq. (5)), since the ratio of active sites to Cr(VI) concentration is increased (Li et al., 2008). For a Cr(VI) concentration of 3 $mg \cdot L^{-1}$, this interaction effect is less perceptible since the ratio of active sites to Cr(VI) concentration is high whatever the concentration of nZVI.

Both the final pH and ORP values were affected by the nZVI concentration (U_1) and nZVI surface modification (U_2) (Fig. A.6). Solutions were more alkaline and reductive for high nZVI concentration or for CMC-modified nZVI. Since no effect of or interaction between the factors Cr(VI) concentration and NO_3^- concentration was noticed, only the nZVI concentration and surface modification managed independently the long-term physicochemical conditions of the solution.

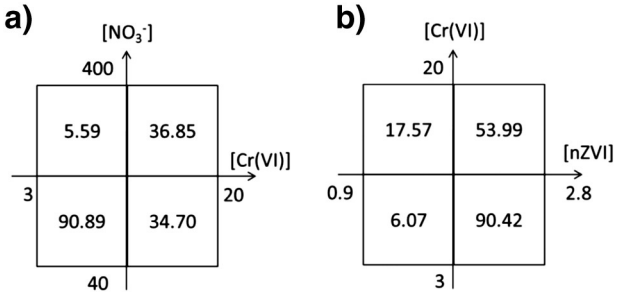

Fig. 4. Interaction effects of Cr(VI) concentration (U_3) and NO_3^- concentration (U_4) (a), and nZVI concentration (U_1) and Cr(VI) concentration (U_3) (b) on the response molar ratio of non-chlorinated transformation product to initial TCE (Y3).

5. Conclusion

Cr(VI) and NO_3^-, at concentration levels examined in this study (tens of $mg \cdot L^{-1}$), could affect the reactivity of nZVI towards TCE. However, in the present work, satisfactory TCE removals were achieved for the lowest concentration levels tested, i.e., 3 $mg \cdot L^{-1}$ of Cr(VI) and 40 $mg \cdot L^{-1}$ of NO_3^-, either by increasing the concentration of nZVI, as expected, or by modifying nanoparticle surface with CMC, which also has the advantage of improving the mobility of nZVI through the aquifer. Moreover, the negative effects of the co-pollutants at the highest concentration levels tested (20 $mg \cdot L^{-1}$ of Cr(VI) and 400 $mg \cdot L^{-1}$ of NO_3^-) can be palliated by combining surface modification with a slight increase in nZVI concentration. Even if a decrease in TCE kinetic rates was observed, the half-life times remained sufficiently short for in-situ applications. For instance, in the presence of 400 $mg \cdot L^{-1}$ of NO_3^- and 20 $mg \cdot L^{-1}$ of Cr(VI), a complete removal of TCE was achieved in about 1 week when using 2.8 $g \cdot L^{-1}$ CMC–nZVI. In addition, taking into account the method detection limits (5 $\mu g \cdot L^{-1}$) and a 10 to 15% experiment uncertainty, the TCE concentration has dropped below 10 $\mu g \cdot L^{-1}$, which is the threshold concentration for groundwater good status that has been fixed in France, according to

the European Water Framework Directive (2000/60/EU, 2006/118/EU). Moreover, TCE concentration is certainly very close to the EPA maximal contaminant level (MCL), which has been set at 5 $\mu g \cdot L^{-1}$. These results are promising in terms of in-situ applications.

Moreover, the reactivity and fate of nZVI particles in groundwaters can also be affected by the presence of non-reducible ionic species, such as SO_4^{2-}, Cl^-, HPO_4^{2-} or HCO_3^- (Agrawal et al., 2002; Liu et al., 2007). Their effects depend on their concentration levels, as for Cr(VI) and NO_3^-. These concentrations are highly site-dependent and can cover a wide range, given that their sources can be natural or anthropic. Hence, it is necessary to characterize groundwaters as finely as possible before treatment. The methodology proposed here could help optimize the appropriate injection parameters, through preliminary laboratory experiments, taking into account the geochemistry and the complexity of the groundwater studied.

Acknowledgments

This research was supported by the French National Agency for Research (ANR, NANOFREZES project), the European Union funds (FEDER), a PhD grant (PACA region, France), Hyphen Consulting, and the ECCOREV Research Federation. The authors thank Nicolas Bongard (PerkinElmer) and Christian Missitch (COFALAB) for their friendly technical assistance, and Nanoiron and Aquatest for NANOFER samples, for letting us use their dispersing/coating unit and for their assistance. The authors thank Prof. Gregory V. Lowry for his valuable suggestions on the experimental design. Lastly, we are also grateful to Patrick Fournier and Claude-Hélène Mignard for their useful linguistic corrections and suggestions.

Appendix A. Supplementary data

Supplementary data to this article can be found online at http://dx.doi.org/10.1016/j.scitotenv.2014.02.043.

References

Agrawal A, Ferguson WJ, Gardner BO, Christ JA, Bandstra JZ, Tratnyek PG. Effects of carbonate species on the kinetics of dechlorination of 1,1,1-trichloroethane by zero-valent iron. Environ Sci Technol 2002;36(20):4326–33.
Alowitz MJ, Scherer MM. Kinetics of nitrate, nitrite, and Cr(VI) reduction by iron metal. Environ Sci Technol 2002;36(3):299–306.
Arnold WA, Roberts AL. Pathways and kinetics of chlorinated ethylene and chlorinated acetylene reaction with Fe(0) particles. Environ Sci Technol 2000;34(9):1794–805.
Chen J-L, Al-Abed SR, Ryan JA, Li Z. Effects of pH on dechlorination of trichloroethylene by zero-valent iron. J Hazard Mater 2001;83(3):243–54.
Cho H-H, Park J-W. Effect of coexisting compounds on the sorption and reduction of trichloroethylene with iron. Environ Toxicol Chem SETAC 2005;24(1):11–6.
Choe S, Chang Y-Y, Hwang K-Y, Khim J. Kinetics of reductive denitrification by nanoscale zero-valent iron. Chemosphere 2000;41(8):1307–11.
Cirtiu CM, Raychoudhury T, Ghoshal S, Moores A. Systematic comparison of the size, surface characteristics and colloidal stability of zero valent iron nanoparticles pre- and post-grafted with common polymers. Colloids Surf Physicochem Eng Asp 2011;390(1–3):95–104.
Dou X, Li R, Zhao B, Liang W. Arsenate removal from water by zero-valent iron/activated carbon galvanic couples. J Hazard Mater 2010;182(1–3):108–14.
Dries J, Bastiaens L, Springael D, Agathos SN, Diels L. Combined removal of chlorinated ethenes and heavy metals by zerovalent iron in batch and continuous flow column systems. Environ Sci Technol 2005;39(21):8460–5.
Farrell J, Kason M, Melitas N, Li T. Investigation of the long-term performance of zero-valent iron for reductive dechlorination of trichloroethylene. Environ Sci Technol 2000;34(3):514–21.
He F, Zhao D, Paul C. Field assessment of carboxymethyl cellulose stabilized iron nanoparticles for in situ destruction of chlorinated solvents in source zones. Water Res 2010;44(7):2360–70.
Henderson AD, Demond AH. Long-term performance of zero-valent iron permeable reactive barriers: a critical review. Environ Eng Sci 2007;24(4):401–23.
Henn KW, Waddill DW. Utilization of nanoscale zero-valent iron for source remediation—a case study. Remediat J 2006;16(2):57–77.
Jeen S-W, Yang Y, Gui L, Gillham RW. Treatment of trichloroethene and hexavalent chromium by granular iron in the presence of dissolved $CaCO_3$. J Contam Hydrol 2013;144(1):108–21.
Johnson RL, Nurmi JT, O'Brien Johnson GS, Fan D, O'Brien Johnson RL, Shi Z, et al. Field-scale transport and transformation of carboxymethylcellulose-stabilized nano zero-valent iron. Environ Sci Technol 2013;47(3):1573–80.
Kim H-S, Kim T, Ahn J-Y, Hwang K-Y, Park J-Y, Lim T-T, et al. Aging characteristics and reactivity of two types of nanoscale zero-valent iron particles (FeBH and FeH_2) in nitrate reduction. Chem Eng J 2012;197:16–23.
Kumar N. Nano to granular sized zero valent iron for groundwater remediation: physico-chemical and biological mechanisms. [CEREGE]: Aix Marseille University [CEREGE]: Aix Marseille University; 2013.
Li X, Cao J, Zhang W. Stoichiometry of Cr(VI) immobilization using nanoscale zerovalent iron (nZVI): a study with high-resolution X-ray photoelectron spectroscopy (HR-XPS). Ind Eng Chem Res 2008;47(7):2131–9.
Li S, Fang Y-L, Romanczuk CD, Jin Z, Li T, Wong MS. Establishing the trichloroethene dechlorination rates of palladium-based catalysts and iron-based reductants. Appl Catal B Environ 2012;125:95–102.
Liu Y, Majetich SA, Tilton RD, Sholl DS, Lowry GV. TCE dechlorination rates, pathways, and efficiency of nanoscale iron particles with different properties. Environ Sci Technol 2005;39(5):1338–45.
Liu Y, Phenrat T, Lowry GV. Effect of TCE concentration and dissolved groundwater solutes on NZVI-promoted TCE dechlorination and H_2 evolution. Environ Sci Technol 2007;41(22):7881–7.
Liu T, Rao P, Lo IMC. Influences of humic acid, bicarbonate and calcium on Cr(VI) reductive removal by zero-valent iron. Sci Total Environ 2009;407(10):3407–14.
Liu T, Zhao L, Sun D, Tan X. Entrapment of nanoscale zero-valent iron in chitosan beads for hexavalent chromium removal from wastewater. J Hazard Mater 2010;184(1–3):724–30.
Lv X, Xu J, Jiang G, Xu X. Removal of chromium(VI) from wastewater by nanoscale zero-valent iron particles supported on multiwalled carbon nanotubes. Chemosphere 2011;85(7):1204–9.
Melitas N, Chuffe-Moscoso O, Farrell J. Kinetics of soluble chromium removal from contaminated water by zerovalent iron media: corrosion inhibition and passive oxide effects. Environ Sci Technol 2001;35(19):3948–53.
Mueller NC, Braun J, Bruns J, Černík M, Rissing P, Rickerby D, et al. Application of nanoscale zero valent iron (NZVI) for groundwater remediation in Europe. Environ Sci Pollut Res 2011;19(2):550–8.
Němeček J, Lhotský O, Cajthaml T, et al. Nanoscale zero-valent iron application for in situ reduction of hexavalent chromium and its effects on indigenous microorganism populations. Sci Total Environ 2013. http://dx.doi.org/10.1016/j.scitotenv.2013.11.105.
Official Journal of the European Union. The EU Water Framework Directive 2000/60/EC of the European Parliament and of the Council, 12.22.2000, OJ L 327/1-73.
Official Journal of the European Union. Groundwater Daughter Directive 2006/118/EC to WFD 2000/60/EC of the European Parliament and of the Council, 12.27.2006, OJ L372/19-31.
Pensini E, Sleep BE, Yip C. Transport of iron particles in the silica aquifers: effect of water chemistry and carboxy-methyl cellulose polymer coatings. AGU Fall Meet Abstr. 53; 2011. p. 1402.
Phenrat T, Saleh N, Sirk K, Tilton RD, Lowry GV. Aggregation and sedimentation of aqueous nanoscale zerovalent iron dispersions. Environ Sci Technol 2007;41(1):284–90.
Phenrat T, Liu Y, Tilton RD, Lowry GV. Adsorbed polyelectrolyte coatings decrease Fe^0 nanoparticle reactivity with TCE in water: conceptual model and mechanisms. Environ Sci Technol 2009;43(5):1507–14.
Ponder SM, Darab JG, Mallouk TE. Remediation of Cr(VI) and Pb(II) aqueous solutions using supported, nanoscale zero-valent iron. Environ Sci Technol 2000;34(12):2564–9.
Reinsch BC, Forsberg B, Penn RL, Kim CS, Lowry GV. Chemical transformations during aging of zerovalent iron nanoparticles in the presence of common groundwater dissolved constituents. Environ Sci Technol 2010;44(9):3455–61.
Roberts AL, Totten LA, Arnold WA, Burris DR, Campbell TJ. Reductive elimination of chlorinated ethylenes by zero-valent metals. Environ Sci Technol 1996;30(8):2654–9.
Saleh N, Sirk K, Liu Y, Phenrat T, Dufour B, Matyjaszewski K, et al. Surface modifications enhance nanoiron transport and NAPL targeting in saturated porous media. Environ Eng Sci 2007;24(1):45–57.
Schlicker O, Ebert M, Fruth M, Weidner M, Wüst W, Dahmke A. Degradation of TCE with iron: the role of competing chromate and nitrate reduction. Ground Water 2000;38(3):403–9.
Schrick B, Hydutsky BW, Blough JL, Mallouk TE. Delivery vehicles for zerovalent metal nanoparticles in soil and groundwater. Chem Mater 2004;16(11):2187–93.
Scott TB, Popescu IC, Crane RA, Noubactep C. Nano-scale metallic iron for the treatment of solutions containing multiple inorganic contaminants. J Hazard Mater 2011;186(1):280–7.
Sohn K, Kang SW, Ahn S, Woo M, Yang S-K. Fe(0) nanoparticles for nitrate reduction: stability, reactivity, and transformation. Environ Sci Technol 2006;40(17):5514–9.
Song H, Carraway ER. Reduction of chlorinated ethanes by nanosized zero-valent iron: kinetics, pathways, and effects of reaction conditions. Environ Sci Technol 2005;39(16):6237–45.
Suzuki T, Moribe M, Oyama Y, Niinae M. Mechanism of nitrate reduction by zero-valent iron: equilibrium and kinetics studies. Chem Eng J 2012;183:271–7.
Wang W, Zhou M. Degradation of trichloroethylene using solvent-responsive polymer coated Fe nanoparticles. Colloids Surf Physicochem Eng Asp 2010;369(1–3):232–9.
Wang W, Zhou M, Jin Z, Li T. Reactivity characteristics of poly(methyl methacrylate) coated nanoscale iron particles for trichloroethylene remediation. J Hazard Mater 2010;173(1–3):724–30.
Xu Y, Zhao D. Reductive immobilization of chromate in water and soil using stabilized iron nanoparticles. Water Res 2007;41(10):2101–8.
Yang GCC, Lee H-L. Chemical reduction of nitrate by nanosized iron: kinetics and pathways. Water Res 2005;39(5):884–94.
Zhang W. Nanoscale iron particles for environmental remediation: an overview. J Nanopart Res 2003;5(3–4):323–32.